ISSN: 2710-0588

Study on the Properties of Waste Stone Powder-clay Slurry based on the Influence of Filter Press

Xinming Chen[1,2,3], Jiaojiao Chen[1,2], Huazhe Jiao[2,3,*], Dongbing Li[1,3], Zhi Yang[1,4], Jie Wang[1,3,4]

[1] Henan Provincial Key Laboratory of Green and Efficient Mining and Comprehensive Utilization of Mineral Resources, Henan Polytechnic University, Jiaozuo 454150, China

[2] School of Civil Engineering, Henan Polytechnic University, Jiaozuo 454150, China

[3] Collaborative Innovation Center for Coal Safety Production and Clean and Efficient Utilization, Jiaozuo 454150, China

[4] School of Civil and Resource Engineering, University of Science and Technology Beijing, 100083, Beijing, China

[*]Corresponding Author

Abstract

A grouting material pressure effect simulation device (FSD) was used to study the performance of grout considering grouting pressure, slurry rheology, clay ash, slurry concentration and particle size composition of waste stone powder (FSD influencing factors). After the effect of filter pressing, the alkaline environment of the slurry became stronger, the number of active particles increased, and the $CaCO_3$ and clay crystals were fully agglomerate, and the degree of crystallization increased. The cation exchange capacity increased, and the formation of calcium-silicon-aluminum matrix phase and aluminosilicate aggregates increased. The surface water between the matrix particles supports the crystal layer, and the plastic viscosity and yield stress are reduced. The free calcium oxide decreased, and the consolidation shrinkage rate after slurry hardening was less than 1%. The water-cement ratio is reduced, and the total time for slurry to be poured into the fracture to consolidate and form a mold and intermittent is shortened. The use of waste stone powder and clay in the coal mine grouting industry can not only reduce project costs, but also reduce soil erosion and soil pollution.

Keywords

Waste Stone Powder; Clay; Slurry; Filter Press Effect; Grouting Performance; Development Mechanism.

1. Introduction

Waste stone powder and clay materials can be used locally, and the cost is lower than that of other grout materials [1]. In particular, waste stone powder, as a common industrial waste of stone products, is widely distributed throughout the country [2], and if it is not reused, it can cause extremely serious environmental problems. Even if the soil is reused, it is often accompanied by mechanical mixtures such as clay and organic matter [3], which is contrary to the concept of green material development advocated by the state.

Ga et al. found that the nucleation effect provided by limestone powder particles can improve the strength activity of clay [4]. Bayesteh et al. studied stone powder as a cost-effective additive and found that the addition of 20% stone powder eliminated the negative effects of water and increased the strength of clay-based specimens [5]. Dixit et al. also used 30% waste clay as a

ISSN: 2710-0588

substitute for stone powder filler in ultra-high-performance concrete (UHPC), and isothermal calorimetry proved that clay has a strong nucleation effect [6]. However, after slurry grouting made of clay, it has high plastic strength, water resistance, and dispersion [7].

Clay grouting is cheap, endothermic, cooling, and coal-packed. The use of pure clay grouting can promote the regeneration of coal seam roof and floor, ensure the safety of goaf, and improve the coal mining rate. Based on this, Zhu Yanguang effectively blocked the fissure channel in the goaf and ensured the safe mining of the 3103 fully mechanized mining face [16]. However, a large number of studies have shown [8-15] that adding an appropriate amount of stone powder, cement and other substances can improve the strength characteristics of pure clay grouting, shorten the gel time, and become more superior, while reducing the project cost and environmental pollution.

Because most of the waste stone powder produced by machine-made sand in stone processing in China is collected through vacuum dust collection devices [17], it is convenient and fast, but it will be doped with clay particles, and if it is used to prepare cement-based concrete, it will affect the workability of concrete due to adsorption of superplasticizers and irregular particle shape [18, 19]. Therefore, in order to solve the problem of waste stone powder accumulation generated by the stone processing industry, this paper considers mixing such stone powder waste into clay material cementitious slurry, and using pressure grouting method to fill the fracture zone of coal and rock seam as a technical solution for anti-seepage reinforcement of industrial activities.

2. Trial

2.1. Test Samples

Waste stone powder: taken from the waste stone powder accumulated in a mining processing plant in Shanxi, with calcite mineral as the main component, it is calcium carbonate rock powder, with an external surface area of 580.77 m^2/g, an average particle size of 1.58 μm, a Mohs hardness of 3.2~4.2, a loss on ignition of 46.97%, and a water requirement ratio of 86%.

Clay: standard for construction soil, purchased from Kangtai Mineral Products Processing Plant, Lingshou County, Hebei Province, the main mineral composition is kaolinite, with a clay content of 74.6%, a free expansion rate of 27.5%, and a deformation modulus of 40 MPa.

Water: Clean tap water. The test sample list and composite slurry are shown in Fig. 1.

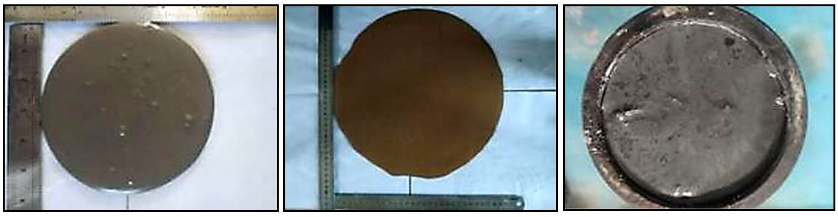

(a)Waste stone slurry (b) Clay slurry (c)Compound slurry

Fig. 1 Single and composite slurry of waste stone powder and clay

The chemical composition of the samples was determined by X-ray fluorescence (XRF) and the results are shown in Table 1. As can be seen from Table 1, waste stone powder and clay are rich in aluminosilicate minerals, the main chemical components are SiO_2 and Al_2O_3, and the naturally occurring aluminosilicate minerals can promote the formation of composite materials with a number of excellent physical and mechanical properties, such as high strength, high hardness, high cohesiveness, and high durability [19, 20]. The CaO content in waste stone powder is much greater than that in clay, and the amount of Fe_2O_3, Na_2O, K_2O, MgO, TiO_2 and SO_3 in the two is small and similar.

ISSN: 2710-0588

Table 1. Chemical composition of Waste stone powder and clay

Material	Chemical composition/Wt%									
	SiO_2	Al_2O_3	Fe_2O_3	Na_2O	K_2O	CaO	MgO	TiO_2	SO_3	CO_2
Clay	49.65	28.70	3.45	0.38	0.44	0.63	3.16	0.90	0.04	0.02
Stone powder	34.05	11.89	2.47	3.32	3.81	36.37	1.35	0.47	0.23	0.03

The types and sizes of minerals in the samples were analyzed qualitatively and quantitatively by X-ray diffractometer (XRD) (Mastersizer 2000). The processed XRD analysis patterns processed by Jade software are shown in Fig. 2, and the particle size analysis results of particle size composition are shown in Fig. 3. As can be seen from Fig. 2, the main diffraction peak of waste stone powder is calcite ($CaCO_3$), the rest of the peaks are quartz (SiO_2), albite ($NaAlSi_3O_8$), potassium feldspar ($KAlSi_3O_8$) and other materials, the main clay diffraction peak is kaolinite ($Al4[Si_4O_{10}](OH)_8$), and the rest of the peaks are illite (K). <1Al_2 [$(Al,Si)Si_3O_{10}$ $(OH)_2{\cdot}nH_2O$]), Muscovite ($K[Al_2[AlSi_3O_{10}](OH)_2$) and montmorillonite ($Al_4Si_8O_20(OH)_4{\cdot}nH_2O$), quartz ($SiO_2$) and other substances. As can be seen from Figure 3, more than 98% of the particles with a particle size of less than 75 μm are contained in the stone powder material, and more than 61% of the particles with a particle size of less than 6.2 μm are contained in the clay material.

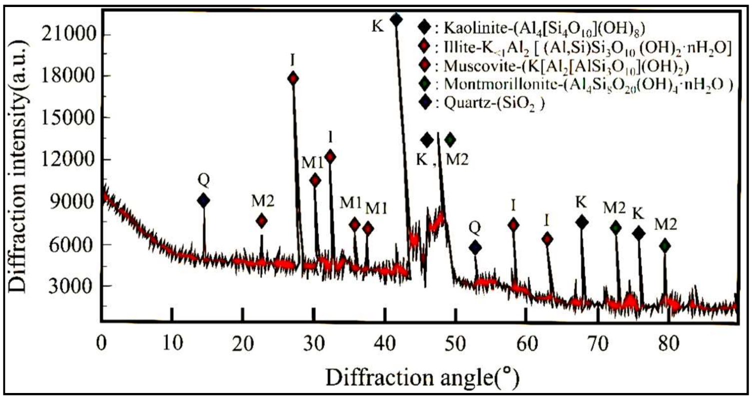

(a)

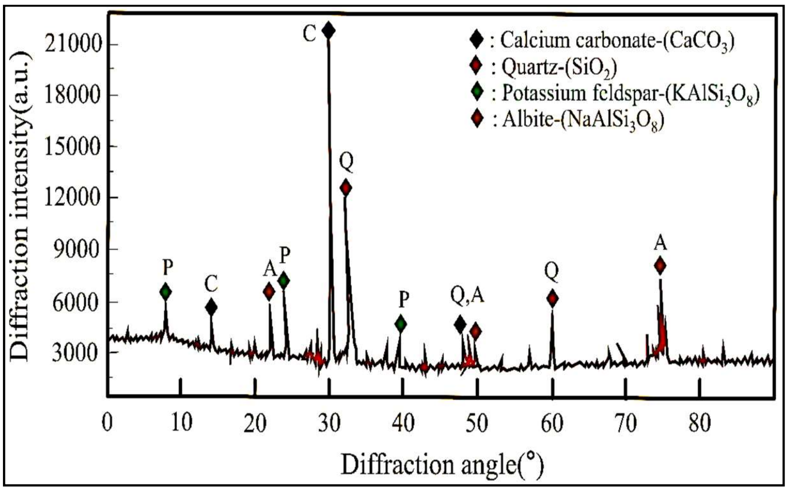

(b)

Fig. 2 XRD analysis. (a) waste stone powder (b) clay

The mineral composition of expansive clay in waste stone powder was determined according to the "Methylene Blue Test Standard Regulations" (BS-EN 933-9:1999), and the MBVF value

ISSN: 2710-0588

was slightly greater than 1.4 and did not exceed the standard specification, and the particles qualitatively contained a small amount of expansive clay. Expansive clay has a strong cation exchange capacity, and the viscosity and strength of expansive clay increase significantly after adsorption of water molecules [21, 22], and the pulping rate is very high as a high-quality slurry clay [23]. Therefore, the slurry contains a small amount of expansive clay, which is conducive to the development of slurry properties[24].

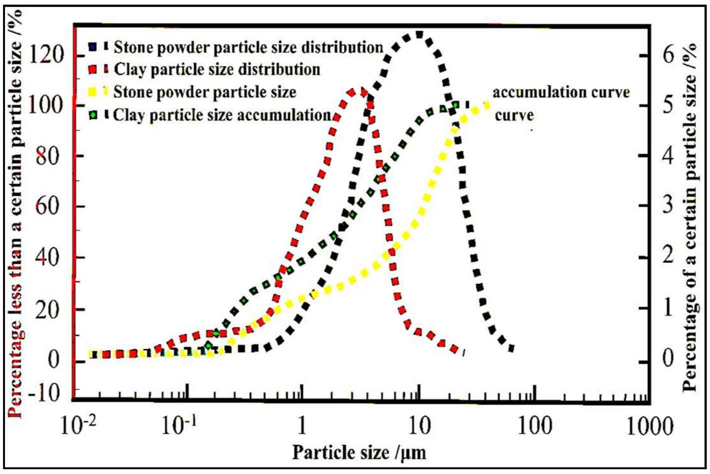

Fig. 3 Particle size distribution and accumulation rate composition curves of waste stone powder and clay XRD analysis.

The 7 d and 28 d activity index (compressive strength ratio) and fluidity ratio of waste stone powder and clay were tested by using an open tilting press (J23-100 type) and a cement mortar fluidity tester (NLD-3 type), with reference to the "Cement Mortar Strength Test Method (ISO Method)" (GB/T 17671-2021). The activity index values of waste stone powder and clay materials increased more and more with time[25].

Table 2. Comparison of slurry and test slurry

Slurry type	Waste stone powder/g	Clay/g	Water/mL
Contrast slurry①	600	-	300
Contrast slurry②	-	600	300
Test slurry	300	300	300

In summary, the physical and mechanical properties of the waste stone powder and clay samples summarized in the test are shown in Table 3.

Table 3. Physical and mechanical properties of waste stone powder and clay samples

Material	MBV_F	Activity index/%		Fluidity ratio/%	Specific surface area/m²/g	Viscosity /mPa·s	Specific gravity/g/cm³
		7d	28d				
Clay	-	90.75	98.17	95.22	651.45	55.8	1.84
Stone powder	14.2	65.44	78.84	89.71	580.77	32.4	2.51
Material	Severe degree/N/m³	Pore compare	Water content/%	Liquid index	Plasticity index	Cohesion/KPa	Internalfrictionangle/°
Clay	1.80	0.32	37.55	178.76	200.05	69.35	21.5
Stone powder	2.46	0.47	0.65	-	-	-	-

ISSN: 2710-0588

2.2. Experimental Design

Table 4. Combination table of waste stone powder-clay slurry level and influencing factors

Level	Influencing factors		
	A Grout pressure intensity/MPa	B Particle size of waste stone powder/μm	C Ratio of waste stone powder to clay content
1	0.5	150	1:1
2	1.5	75	1:1.5
3	3.5	48	1:2
4	5.5	38	1:2.5
5	7.5	25	1:3
6	9.5	23	1:3.5
7	-	0	1:4
8	-	-	1:4.5
9	-	-	1:5

Note: 0 is not screened original waste stone powder.

Table 5. Orthogonal table of waste stone powder-clay slurry mix ratio design and analysis of some results

Experimental group	A	B	C	compressive strength/MPa	Experimental group	A	B	C	compressive strength/MPa
①	1.5	150	1:3	26.4	㉑	1.5	38	1:3.5	25.6
②	0.5	150	1:1	24.2	㉒	5.5	0	1:3	36.8
③	5.5	25	1:1	34.3	㉓	1.5	25	1:2	25.5
④	7.5	48	1:1	33.7	㉔	5.5	23	1:4	37.4
⑤	3.5	48	1:2	30.5	㉕	3.5	23	1:1	31.8
⑥	3.5	38	1:3.5	31.7	㉖	1.5	23	1:5	27.4
⑦	3.5	0	1:4.5	31.5	㉗	5.5	48	1:5	34.6
⑧	7.5	0	1:5	35.1	㉘	1.5	75	1:1.5	25.5
⑨	5.5	150	1:3.5	30.4	㉙	3.5	150	1:5	23.2
⑩	7.5	23	1:1.5	34.2	㉚	7.5	38	1:4.5	39.1
⑪	5	75	1:2.5	30.2	㉛	0.5	75	1:4	22.5
⑫	1	48	1:2.5	26.4	㉜	9.5	25	1:5	37.6
⑬	1	0	1:2	25.9	㉝	5.5	38	1:2.5	29.3
⑭	1	25	1:4.5	30.7	㉞	7.5	25	1:3	31.5
⑮	4	75	1:2	33.2	㉟	7.5	150	1:4	30.2
⑯	1	23	1:3	29.2	㊱	0.5	38	1:1.5	26.6
⑰	2	48	1:4.5	25.8	㊲	3.5	75	1:3.5	32.5
⑱	6	23	1:3.5	36.7	㊳	3.5	25	1:2.5	34.6
⑲	6	150	1:1.5	32.7	㊴	9.5	48	1:3	38.7
⑳	6	38	1:2	34.3	㊵	9.5	75	1:4.5	36.2

Note: 0 is not screened original waste stone powder.

ISSN: 2710-0588

The grouting pressure, the particle size composition of the slurry waste stone powder and the rheology of the slurry, the ash content of the slurry clay and the concentration of the slurry are all factors affecting the pressure effect of the filter press device, and the rheology of the slurry, the ash content of the slurry clay and the concentration of the slurry are determined by the dosage ratio of the waste stone powder and the clay. In order to explore rigorously and conduct a comprehensive experiment, the initial influencing factors and horizontal combinations of experimental design are shown in Table 4. As can be seen from Table 4 each influencing factor has multiple variables, and it is cumbersome and difficult to consider controlling the change of each single factor variable and the rest unchanged. The SPSS-AU system software was used to realize the orthogonal experimental design[26], and some representative level combinations were selected according to the Galois theory for experiments to find out the optimal level combinations[27]. Based on the orthogonal experimental design principle, the final slurry mix design orthogonal table L40 (6^1X7^1X9^1) and some results analysis are shown in Table 5.

2.3. Test Process

2.3.1. The Value of the Filter Press Effect

Combined with the actual on-site filter press grouting process, we cooperated with machinery manufacturers to design a set of filter pressure effect simulation device (FSD). Fig. 5 shows the FSD simulation test equipment and its samples.

(a)WAW-600 material testing machine (b)Data acquisition system (c)Filter press effect mold

(d)Waste stone powder-clay slurry stone body test block

Fig. 4 Filter press effect test equipment and waste stone powder-clay slurry stone body samples

When pressure is applied to the slurry, bottom water molecules are percolated out of the slurry, forming a filter cake with a thickness of L[28], as shown in Fig. 6(a). The cake irregular channels in the filter press model are simplified into vertical thin tube channels parallel to each other, as shown in Fig. 6(c), and specify: a. The inner surface area of the tube channel is equal to all the surface area of the cake particles. b. The tube flow space is the pore volume of the filter cake. The derivation process of the theoretical value required for the grouting test is as follows:

ISSN: 2710-0588

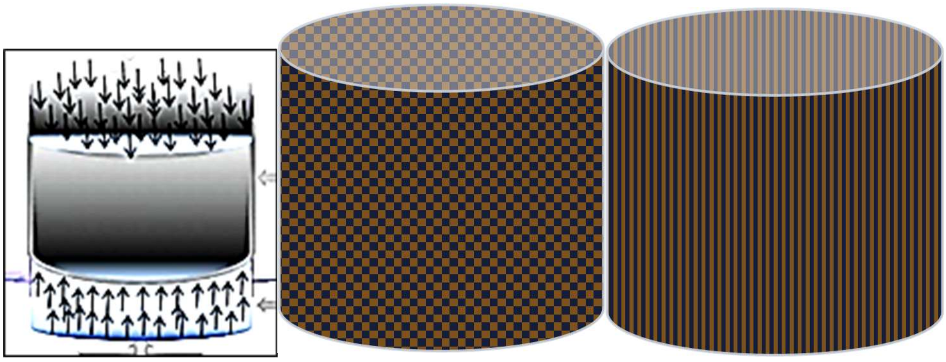

(a) (b) (c)

Fig.5(a) Analysis of filt ration press principle, (b) simplified model of particles inside the filter cake and (c) simplified model of parallel vertical thin tube channel

A. Filter cake thickness (dehydration): calculate the integral number of slurry and the volume of suspended liquid, and derive the theoretical value required for the test.

$$\varphi = V_S/(V_W + V_S) \quad (1)$$

$$L = \varphi q/(1-\varepsilon-\varphi) \quad (2)$$

$$q = V/A \quad (3)$$

where: φ is the integral number of slurry, V is the volume of water in the slurry, V solid is the volume of solid in the slurry, V is the amount of filtrate obtained at the moment, L is the thickness of the filter cake, A is the inner diameter area of the slurry reservoir, ε is the porosity of the filter cake, and q is the amount of filtrate passing through the unit area.

B. Filter press effect application time: assuming that the diameter of the tube channel is de, the pore volume of the bed is ε, the surface area of the particles per cubic meter of the bed is au, and the surface area of the particles is a.

$$d_e = 4\varepsilon/a_u = 4\varepsilon/a(1-\varepsilon) \quad (4)$$

Ignoring the gravitational effect of the slurry, the density of the slurry is, the flow velocity of the thin tube is, and the length of the bed after simplifying it to the thin tube channel. When the flow rate is low, the bed Reynolds number is less than 2:

$$R_e = d_e u_1 \rho/4\mu = \rho u/a\mu(1-\varepsilon) \quad (5)$$

where μ is the viscosity of the slurry. The model parameter λ' is measured by the experiment:

$$\lambda' = \lambda L_e/8L = K/R_e \quad (6)$$

Syntagonical formula (4)~(8) Conzeni equation, in the process of dehydration and separation of slurry, the approximate filtration constant K is taken as 5, and the Conzeni formula is deformed into a filtration speed formula, and the expression is:

ISSN: 2710-0588

$$u = \varepsilon^3 \Delta P / 5a^2 (1-\varepsilon)^2 \mu L \tag{7}$$

$$T = V_L - V_P - V_C / u \tag{8}$$

In the formula: P is the grouting pressure, L is the thickness of the filter cake at the grouting time, T is the total time of slurry dehydration, V suspension is the volume of the suspension[29], V cake is the volume of the filter cake, and V body is the pore volume of the suspension.

2.3.2. Performance Testing

(a)Steps 1~3 (b)Step 4 (c)Step 5 :Reset the abrasive (d)Step 6: Ready for next use

Fig. 6 Test operation process based on the influence of filter press effect

3. Results and Discussion

3.1. The Filter Pressure Effect Affects the Working Performance of Waste Stone Powder-clay Slurry

As shown in Fig. 6(a), the shear stress τ of the six groups of slurries increases with the increase of the shear rate γ, and the increase rate is different before and after the effect of the filter press. Fig. 6(b) also shows that the apparent viscosity η_a of the six groups decreases with the increase of shear rate, and the apparent viscosity value of the FEL decreases rapidly in the initial shear rate segment and gradually slows down with the increase of shear rate. After the slurry is formed, the gelling between various particles inside is caused by the collision and adsorption of opposite charges, van der Waals gravitation, etc. There is a large amount of cementitious structure in the slurry, which creates a large resistance to the rotor[30]. After the rotor is running, the rotor is subjected to shear forces, and the cementitious structure is constantly destroyed. FEL, part of the cementitious structure formed by the slurry disperses and disintegrates, and the free water in the gelatinous condensate is released. The slurry is dominated by the original cementitious structure, and the dispersed particles coexist with some cementitious structures that are too strong to be dispersed. It is precisely these structures of the slurry that cause it to produce resistance, but this resistance is smaller than the original cementitious structure, and a small external force can produce flow, so the yield stress is small. Since most of the cementitious structures are disintegrated, with the increase of rotation speed, there are not many cementitious structures that can be destroyed, and the shear stress changes are relatively stable, so the rheological curve appears relatively gentle. At the same time, due to the disintegration of the cementitious structure, free water is released, and the relative solid concentration of the slurry decreases, and the viscosity decreases.

The Bingham rheological equation of the samples can be obtained by linear fitting of the least-squares method for the corresponding shear stress values at each shear rate of the six groups of samples.2.1 The filter pressure effect affects the working performance of waste stone powder-clay slurry.

ISSN: 2710-0588

Based on NBF and BF, the test samples of group (30) were selected. The infrared spectrometer FTIR (Spectrum 3 type) was used to test the group structure and characteristic bands of the stone body after 28 days of curing. Sampling, cleaning, adhesive and coating, SEM and the attached EDS scanning electron microscope (Horiba 7021-H) were used to test the topography characteristics and elemental composition. The ultramicrotome was used to section, the probe was mounted, the laser beam and spot were adjusted, the sliced samples were mounted, and the morphology and structure of the stone body in the permeation test water were tested for 28 days by AFM atomic force microscope (Bruker Dimension type). The specimen is then ground into powder and subjected to thermogravimetric analysis TG-DTG (STA 449F3 type) for testing[31]. Combined with inductively coupled plasma atomic emission spectrometer (Plasma ICP-OES2000) and ion chromatography analyzer (ICS-600), the concentration of calcium and aluminum ions in the test aqueous solution was detected.

$$①-\ A+B+C: \tau = 29.33 + 0.7134\gamma$$
$$①-B+C: \tau = 64.35 + 1.812\gamma$$
$$⑮-A+B+C: \tau = 12.994 + 0.4611\gamma$$
$$⑮-B+C: \tau = 21.57 + 1.026\gamma$$
$$㊵-A+B+C: \tau = 17.47 + 0.8554\gamma$$
$$㊵-B+C: \tau = 37.28 + 1.824\gamma$$

As can be seen from Table 6, the plastic viscosity and yield stress of the slurry before the influence of the filter press effect (FE) are larger, and the plastic viscosity and yield stress are reduced by FEL. It shows that FEL can greatly improve the rheological properties of slurry.

Table 6. Rheological parameters of waste stone powder-clay slurry

Rheological parameters	Plastic viscosity(Pa·s)	Yield stress(Pa)	R^2
①-A+B+C	0.7134	29.33	0.9413
①-B+C	1.812	64.35	0.9524
⑮-A+B+C	0.4611	12.994	0.9772
⑮-B+C	1.026	21.57	0.9598
㊵-A+B+C	0.8554	17.47	0.9744
㊵-B+C	1.824	37.28	0.9987

concentrate:R=correlation coefficient.

As shown in Fig. 7(c), the initial and final setting times of FEL slurry are shortened by about half compared with FE. The free water in the slurry is removed, and the water-cement ratio is reduced. FEL shortens the total time for slurry injection into the fracture to consolidate and mold formation and intermittent[32], and shortens the gel time. Once the gel rate is determined, the slurry diffusion range is also accurately controlled. As shown in Fig. 7(d), FEL increased the stone formation rate and was basically stable at 100%, and correspondingly, the consolidation shrinkage rate was less than 1% and basically did not shrink. The higher the stone rate, the better the reinforcement effect and the higher the strength [33].

ISSN: 2710-0588

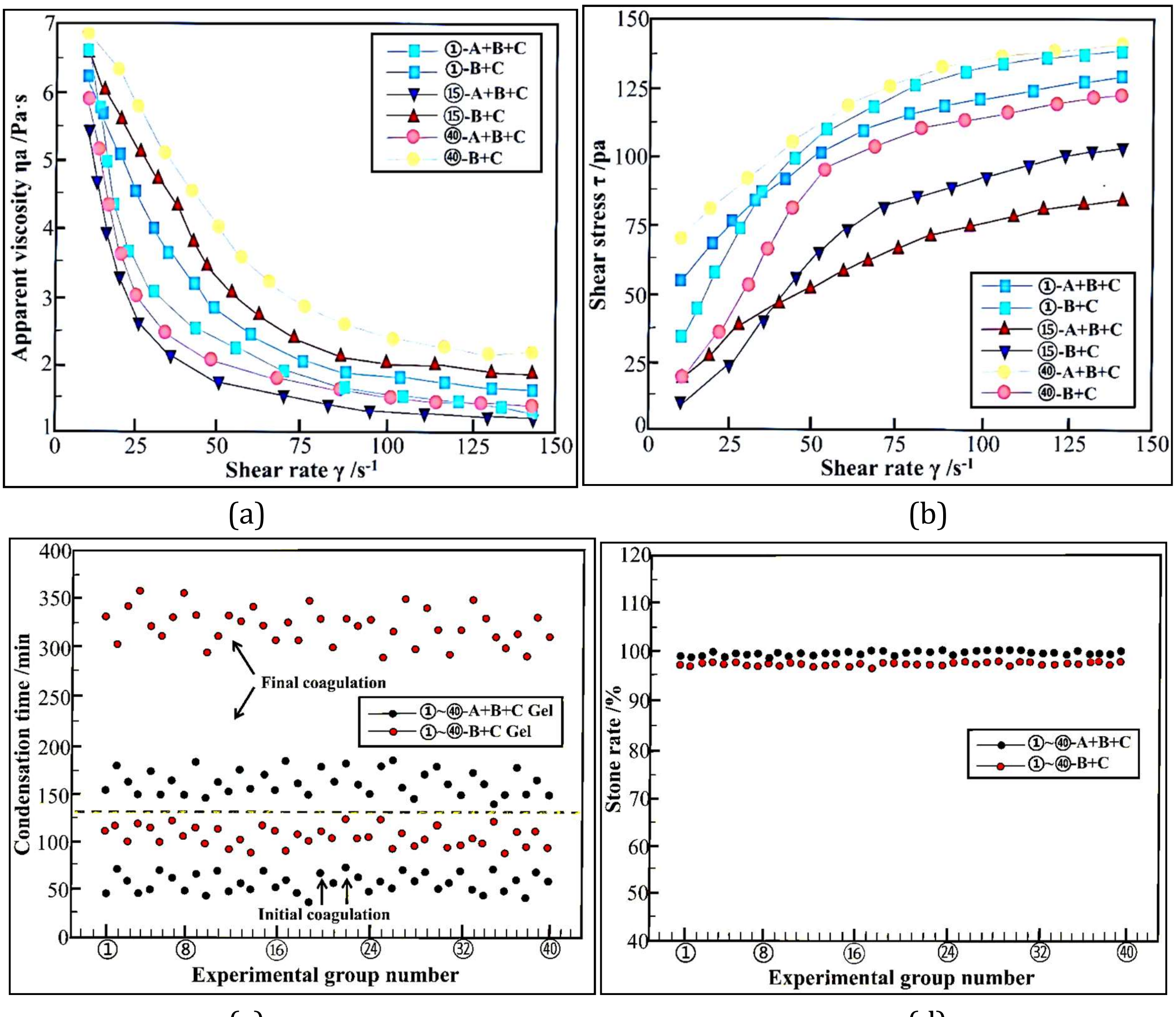

Fig. 7 (a) rheological curve, (b) apparent viscosity curve, (c) gel time plot and (d) firmness dot plot of waste stone powder-clay slurry based on NBF and BF

3.2. The Filter Pressure Effect Affects the Mechanical Properties of Waste Stone Powder-clay Slurry

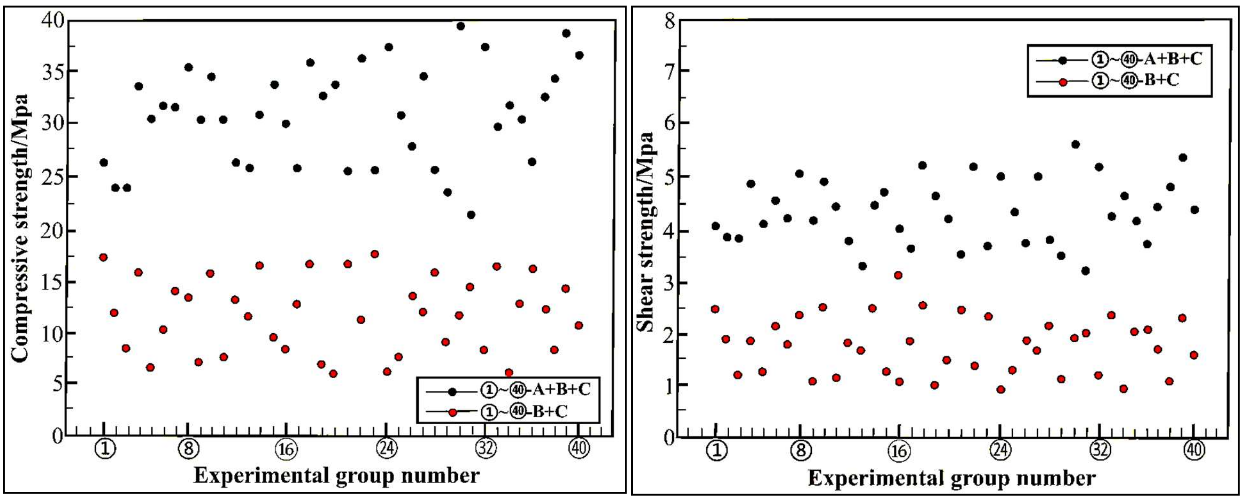

(a) (b)

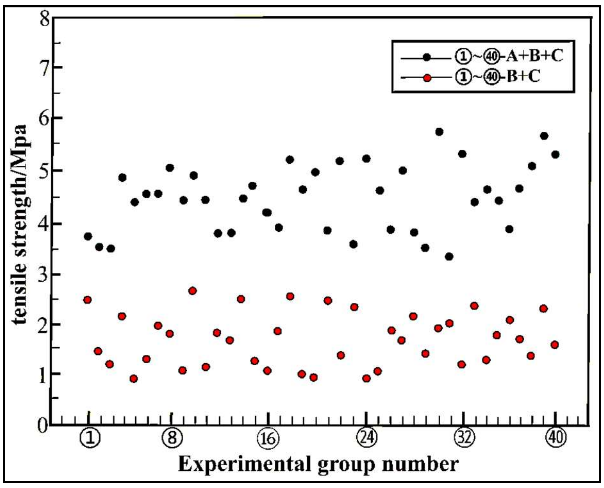

(c)

Fig. 8 Dotplots of (a) compressive strength, (b) shear strength and (c) splitting tensile strength based on NBF and BF waste stone powder-clay slurry

As can be seen from Fig. 8(a)(b)(c), $\sigma_{bc} > \sigma_c \approx \sigma_b$. FEL enhanced the strength of the slurry, and the strength ratio of each strength was greater than the activity index of the monomer. Clay particles are generally highly active, and the active SiO_2 and Al_2O_3 contained in them react with $CaCO_3$ to produce more composite cementitious structures [34]. The activity of stone powder is low, and the strength of monomer mortar is low, and it generally plays a filling role in the slurry. FEL enhanced the chemical action and crystal nucleation of $CaCO_3$ particles in waste stone powder, increased the compactness of the matrix interface transition zone[35], and significantly improved the strength of the stone body.

3.3. The Pressure Effect Affects the Long-term Durability of Waste Stone Powder-clay Slurry

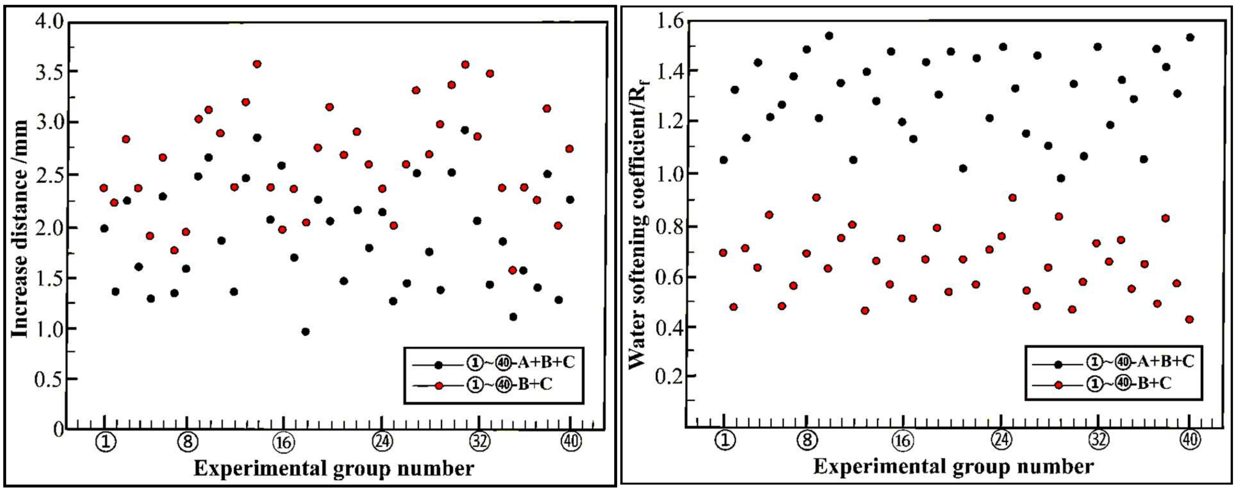

(a) (b)

Fig. 9 (a) stability detection dot plot and (b) Cl-corrosion resistance coefficient dot plot based on NBF and BF waste stone powder-clay slurry

As shown in Fig. 9(a), the volume changes during the coagulation and hardening of the slurry, but the distance increase is less than 4 mm, and the stability test is qualified. The distance change of FEL is controlled within 3 mm, the process of excess free water is removed, the interliquid elements are fully adsorbed and exchanged, the calcium and free calcium oxide contained in the slurry are reduced, the volume changes uniformly after hardening, the

ISSN: 2710-0588

structure is more compact, and there are no cracks in the matrix[36]. As can be seen from Fig. 9(b), the compressive strength ratio of the FEL matrix when immersed in Cl-rich water for 28 days, i.e., the water softening coefficient is the largest, which exceeds 1.0. After the slurry is consolidated, the internal pore connectivity is slightly open, and the external water can easily enter. After the consolidation of the FEL slurry, the pores are compressed to a very small size per unit volume, the apparent density is amplified, the water absorption is affected, the pores are closed, the matrix is denser, and the water resistance and impermeability are superior.

4. Conclusion

The waste stone powder and clay particles are very small, both of which are less than 75 μm, so the slurry can be easily pumped into the fine cracks and pores of the rock and soil layer, and the stone body does not shrink, and the water plugging rate can reach more than 97%. The waste stone powder-clay slurry has water dilution resistance, high dispersion and high controllable rheology, and the stone body has high strength and good stability.

(1) FEL, the formation of aluminosilicate phase increases. The σbc of the matrix was greater than 20 MPa, σc was greater than 3 MPa, and σb was greater than 3 MPa. The rheological properties of the slurry are greatly improved. The consolidation shrinkage rate after slurry hardening is less than 1%, the gel time of pouring into the fracture is shortened, the stone rate is increased, and the corrosion resistance and softening coefficient are improved.

(2) FEL, the slurry generates structural groups with higher cohesion and higher strength, and the bond strength with the base layer of the irrigated soil is improved. The crystallization degree of $CaCO_3$ and clay crystals in the waste stone powder increased, resulting in the excellent development of the mechanical properties and durability of the stone body. FEL, the dispersion of clay particles is more stable, less prone to coagulation and precipitation, and the matrix forms a large number of very homogeneous and dense cohesive structures.

(3) There is no influence of excess free water, KH and AH do not lose crystal water, and the viscosity and cohesion of KH, AH, AO, SO and KO are not lost, and Ca· Si· Al-KH· AH· AO· SO· KO glue agglomerate structure. FEL reduces the dissolution of Al3+ and Ca2+, and promotes the absence of free Ca^{2+} in the matrix, so that the strength of the waste stone powder-clay slurry is more and more similar to that of the cement slurry.If you follow the “checklist” your paper will conform to the requirements of the publisher and facilitate a problem-free publication process.

References

[1] NongY Y. Development and application performance of polyvinyl formaldehyde-montmorillonite composite particles. Master’s thesis, China University of Geosciences (Beijing), China, 2021 (in Chinese).

[2] Liang Y, Zhuang Y, Chen Y F, et al. Materialpruefung: Werkstoffe und Bauteile, Forschung Prufung Anwendung, 2018, 60(11), 111260.

[3] Xu S, Zeng L, Li C ,et al. Fresenius Environmental Bulletin, 2018, 27(6): 4156-4161.

[4] A GA, B BU. Construction and Building Materials, 2021, 284, 122789.

[5] Bayesteh H, Sharifi M. Construction and Building Materials, 2020, 262(3), 120792.

[6] Dixit A, Du H, Pang S D. Construction and Building Materials, 2020, 263, 120250.

[7] Zhang C, Yang J S, Fu J Y, et al. Journal of Central South University, 2019, 26(7): 1863-1873.

[8] ZHU Y G. Coal and Chemical Industry, 2023, 46(03): 111-114+118 (in Chinese).

[9] Su P, Liu F, Yao P, et al. Advances in Civil Engineering, 2021, 2021(10): 1-8.

[10] Zhang J, Li S, Li Z, et al. Construction and Building Materials, 2020, 260(2–3): 119704.

[11] Li Z F, Chen J P, Yang L et al. Chinese Journal of Engineering, 2021, 43(6): 768-777 (in Chinese).

ISSN: 2710-0588

[12] Mashaan N, Yusoff N I M, Saad I. Using Waste Materials in Geotechnical and Pavement Engineering for Sustainable Construction (Sustainability, IF: 2.576 (2019)), 2021.

[13] ROOHBAKHSHAN, Armin, KALANTARI, et al. Annals of the Faculty of Engineering Hunedoara - International Journal of Engineering, 2013, 11(4): 177-180.

[14] Gu J, Moon K, Jegal H, et al. Experimental Investigation of Self-excited Low-swirl Flame Dynamics with Different Blockage Ratios.Journal of The Korean Society of Combustion, 2022.

[15] Guo L, Zhou M, Wang X, et al. Construction and Building Materials, 2022, 328: 126997.

[16] He H, Wang Y, Wang J. Construction and Building Materials, 2020, 250: 118828.

[17] Song N, Wang Q, Wang C, et al. IOP Conference Series Earth and Environmental Science, 2021, 693(1):012097.

[18] Yuguang LI, Hanqing J, Lijuan W. Engineering Technology, 2021(1): 478-481.

[19] Chen W F, Xing Z Q, Wang K X et al. Water Resources and Hydropower Engineering, 2021. 52(5): 196-202 (in Chinese).

[20] Liang J W, Song Z L, Wang X et al. Water Resources and Hydropower Engineering, 2015, 46(10): 133-137 (in Chinese).

[21] Zhu G, Zhang Q, Liu R, et al. Geofluids, 2021, 6613990.

[22] Sakakibara S, Koyama T, Shimizu H. CFD-DEM Simulations for Injection of Cement-Based Grout – The Effect of Rock Fracture Roughness. 2014.

[23] Yin T, Zhang Z, Huang X, et al. Tunnelling and Underground Space Technology, 2021, 111: 103856.

[24] Wang J R, Jing Q S, Liu B et al. Abstract collection of papers of the 2020 academic annual meeting of the Henan Chemical Society, 2020: 1-1 (in Chinese).

[25] Niu R J, Huang P, Li J T, et al. Phosphate Fertilizer & Compound Fertilizer, 2021, 36(9): 38-40. (in Chinese).

[26] Wu X L, Zhang Y Y, Long H M, et al. Science & Technology Vision, 2022(15): 48-51 (in Chinese).

[27] Chen W Y, Zhang Z X, Meng E C, et al. Chinese Journal of the Chinese Ceramic Bulletin, 2023, 42(2): 439-447 (in Chinese).

[28] Yu Y Y, Jing Q S, Yu X H, et al. Mineral Protection and Utilization, 2022, 42(4): 60-67 (in Chinese).

[29] Sun R R, Wang Z, Huang F L, et al. Materials Reports, 2021, 35(Z1): 211-215. (in Chinese).

[30] Cheng G, Fan W, Yu N Y, et al. Rock and Soil Mechanics, 2023(S1): 1-10 (in Chinese).

[31] ZUO X Y. Molecular simulation of carbon dioxide adsorption and diffusion by clay minerals. Master's Thesis, Taiyuan University of Technology, 2019 (in Chinese).

[32] Cui J Q. Study on the influence of clay minerals on pore structure and water absorption characteristics of mudstone. Master's Thesis, Taiyuan University of Technology, 2019 (in Chinese).

[33] Lian B B. Effect of clay mineral content on swelling of rockfall soil under different ion concentrations. Master's Thesis , Fujian Agriculture and Forestry University, 2019 (in Chinese).

[34] Gou K Y. Theoretical study on adsorption characteristics of clay mineral montmorillonite. Master's Thesis , Guangxi University of Science and Technology, 2020 (in Chinese).

[35] Awan A A . Materials, 2021, 14(14), 3829.

[36] Tang M, Yang S, Guo J F, et al. Journal of Building Materials, 2022, 25(02): 191-198 (in Chinese).